

Adaptive variational sinogram interpolation of sparsely sampled CT data

H. Köstler¹, M. Prümmer², U. Rüde¹ and J. Hornegger²
Lehrstuhl für Systemsimulation¹, Mustererkennung²
Friedrich-Alexander University of Erlangen-Nuremberg
91058 Erlangen, Germany

{harald.koestler, pruemmer, ruede, joachim.hornegger}@informatik.uni-erlangen.de

Abstract

We present various kinds of variational PDE based methods to interpolate missing sinogram data for tomographic image reconstruction. Using the observed sinogram data we inpaint the projection data by diffusion. To overcome the problem of contour blurring we consider nonlinear and anisotropic diffusion based regularizers and include optical flow information in order to preserve the sinuodal traces corresponding to object contours in the reconstructed image. We compare our results to a spectral deconvolution based interpolation and show that the method can easily be extended to 3D.

1. Introduction

Tomographic image reconstruction is applied in various fields of medical imaging. Conventional CT scanners and C-arm systems e.g. allow a tomographic reconstruction of a 2D or 3D image of a patient. For the reconstruction, a rotating X-ray device is used to acquire a sequence of angiographic X-ray images. During the rotation around the humans body the attenuated X-ray intensities are observed that are subjected under the condition of the exponential attenuation law. Algorithms like *filtered-backprojection* (FBP) introduced by Feldkamp, Davis and Kress (FDK) [6] allow a 2D or 3D reconstruction using the observed X-ray image sequence. These kind of algorithms underlie the theory of the *fourier-slice-theorem* that implies that at least an acquisition angle of 180 degree – using parallel beam and angle steps as small as possible – is necessary for providing a high image quality of the reconstructed image and avoid streak artifacts. Since the acquisition trajectory of the X-ray source is circular all attenua-

tion coefficients inside the reconstructed image plane – that lies orthogonal to the rotation axis – describe a sinusoidal trace (see Figure 1) in the projection image sequence. The amplitude of the sinusoidal trace of an attenuation coefficient is determined by its distance to the rotation axis. Therefore this projection image sequence is also called *sinogram*. Using a 1D X-ray detector, the horizontal axis in the sinogram corresponds to the projection angle and the vertical axis to the pixel position of the observed X-ray intensity inside the detector.

Unfortunately in some clinical applications like limited angle tomography or cardiac CT the sinogram data is sparse and the reconstructed image will observe various kinds of artifacts. The more uniformly spread along a half or full circular scan the sinogram data is given in small angular steps, the better the image quality of the reconstruction will be.

In this paper we present a new variational approach for sinogram data interpolation prior to reconstruction based on the work of Weickert [12]. In contrast to interpolation prior to reconstruction there are algorithms like Gerchberg-Papoulis (GP) [10] that are iterative procedures for band-limited extrapolation. Haponen [7] performed sinogram extrapolation based on Stackgrams. A hierarchical approach using geometry information can be found in [9]. We see the sinogram as a partial incomplete 2D or 3D image.

2. Interpolation methods

Our key idea comes from video inpainting (cf. e.g. [5]) where several key frames of an image sequence are given and new frames are interpolated in-between. For a 2D CT slice reconstruction we have a 2D sinogram with missing samples along lines (*gaps*) where the gap positions are exactly known. Using the observed

projection data we use diffusion to inpaint the missing sinogram data. High frequencies along the X-ray detector line correspond to structure in the reconstructed object. If we blur the sinuodal traces along the detector line we will also blur the contour of the reconstructed object. Since the shape information of the object is distributed in the whole sinogram image it is preferable to consider all the observed sinogram data for the interpolation. Therefore we regularize additionally along the projection angle axis and use different kind of diffusivity functions that allow us to achieve a smooth interpolation along the sinuodal trace while preserving edges along the detector lines.

The variational approach is compared to the *spectral deconvolution* (SD) algorithm introduced by Til Aach [1],[2] for defect pixel interpolation of flat panel detectors. In our case the defect pixel correspond to the known gaps in the sinogram image.

2.1. Spectral Deconvolution

We have two sets of input: an *observed sinogram* $g(n)$ (of size $N \times \Phi$) - where N is the number of detector pixel and Φ the scan angle - and a gap image mask $w(n)$ that has zero lines at projection angles ϕ where no data is given otherwise it is one. And therefore we can formulate an incomplete sinogram image as follows:

$$g(n) = f(n)w(n), \quad (1)$$

where $f(n)$ is the *ideal sinogram* that we want to find. It would seem easy that all we need is to divide the incomplete sinogram $g(n)$ by the gap mask $w(n)$ in order to obtain $f(n)$. However, a division is not possible as the mask is constituted of zero values of the gaps. Therefore we apply a spectral deconvolution introduced by Til Aach [1],[2].

2.2. Variational Interpolation Approach

In the variational setting the ideal and the incomplete sinograms are considered as functions $f, g : \Omega \rightarrow \mathbf{R}$ in the sinogram domain $\Omega \subset \mathbf{R}^2$ (or $\Omega \subset \mathbf{R}^3$). f is obtained by minimizing the energy functional

$$E(f) = \int_{\Omega} w(x)(g - f)^2 + (1 - w(x))\Psi(s^2) dx, \quad (2)$$

where $x \in \Omega$, $s^2 = |\nabla^k f|^2$ and $k \in \{1, 2\}$. The first term ensures the equivalence of g and f at positions, where the sinogram data is known, and $\Psi : \mathbf{R} \rightarrow \mathbf{R}$ is a regularizing term filling in the missing information. This leads to the Euler-Lagrange equations

$$\begin{aligned} -L(f) &= 0 & \text{if } w(x) = 0 \\ f &= g & \text{if } w(x) = 1 \\ \frac{\partial f}{\partial n} &= 0 & \text{on } \partial\Omega \end{aligned}, \quad (3)$$

with $x \in \Omega$ and the elliptic differential operator $L(f) = \nabla^k \cdot (\Psi'(s^2)\nabla^k f)$. This system of PDEs with Neumann boundary conditions is discretized by finite differences in space and for the nonlinear variants additionally by an explicit Euler forward scheme in time. Afterwards it is solved by either a simple Gauss Seidel iteration or if necessary (to enable a fast transport of the information through large gaps) by a multigrid solver (cf. [11]).

We have implemented various linear regularizers with $\Psi(s^2) = s^2$ such as isotropic harmonic diffusion (IH) $L(f) = \Delta f$, biharmonic diffusion (BI) $L(f) = \Delta^2 f$, and anisotropic harmonic diffusion (AH) $L(f) = \nabla \cdot (D\nabla f)$. The idea for AH is that we try to smooth mainly in the direction of the optical flow (cf. [8]). Therefore the tensor $D = \begin{pmatrix} (u/v)^2 + \alpha_1 & u \\ u & (1 - (u/v)^2) + \alpha_2 \end{pmatrix}$ with $\alpha_1, \alpha_2 > 0$ was constructed using motion information from the left to the right side of a gap approximated by the normalized optical flow vector $(u/v, 1)^T$. v is the size of a gap measured in number of pixels. For 1D optical flow we approximate the spatial resp. temporal derivative g_x and g_t of g by finite differences, where g_t is computed between the two sides of a gap. We have

$$\begin{aligned} u &= 0 & \text{if } g_x = 0 \\ u &= -\frac{g_t}{g_x} & \text{if } g_x \neq 0 \end{aligned}. \quad (4)$$

In higher dimensions we get the optical flow vector by solving a system of PDEs using multigrid.

Note that in 1D the harmonic diffusion would correspond to linear and biharmonic diffusion to cubic spline interpolation, in higher dimensions to using radial basis functions ([3]). In addition to these we tried isotropic nonlinear diffusion (IN) $L(f) = \nabla \cdot (\Psi'(s^2)\nabla f)$ with a Charbonnier diffusivity $\Psi'(s^2) = \frac{1}{1+s^2/\lambda^2}$ and a contrast parameter $\lambda > 0$. More informations about PDE based interpolation methods and their properties can be found in [4], [12], [13].

3. Results

In 2D we implemented the interpolation algorithms using matlab. As a test image we used a slightly modified Shepp-Logan head phantom (size 128x128) depicted in Figure 1. In the incomplete sinogram 66.2% of the points were missing.

For computing the sinogram and the reconstruction we used the matlab functions `radon` and `iradon` doing parallel beam projections. As reconstruction error E_r we measured the L_2 -norm per pixel between the original and the reconstructed image in order to compare the different methods. All subsequent errors values have to be scaled by 10^{-4} .

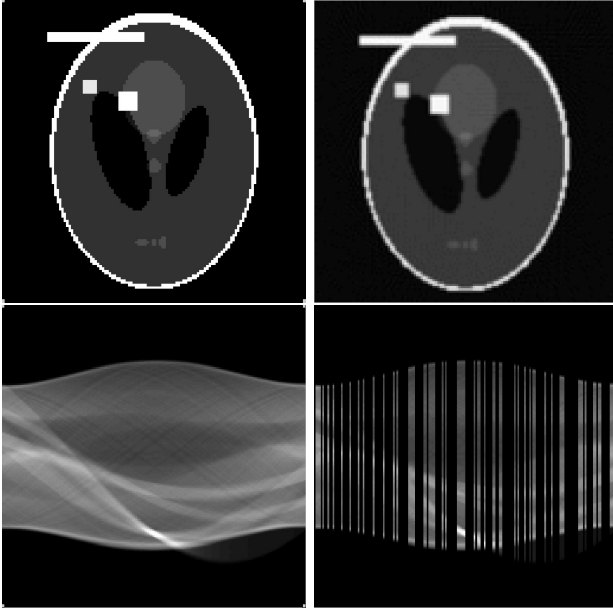


Figure 1. Phantom (top left (TL)), its sinogram (bottom left (BL)), reconstructed image using full sinogram data (top right (TR)) and sinogram with gaps (bottom right (BR)).

The reconstruction error of the original sinogram without gaps was 9.41, the gapped sinogram without interpolation gave 16.0. Simple linear interpolation leads to an error of 9.61. Table 1 shows the errors for different interpolation methods. The parameter α is used to weight the smoothing in different directions, e.g. $(0, 1)$ would be linear interpolation only in y-direction. Note that the time for the reconstruction is 3.45 seconds (on a Pentium M 1400Mhz Laptop).

In Figure 2 some of the interpolated sinograms are shown. One can observe that edges along a detector line is preserved while smoothing along the sinuodal traces. Reconstructed images for different interpolation methods with corresponding magnified image regions can be found in Figures 3 and 4.

For the 3D experiments we used C++. Figure 5 shows the volume rendered 3D phantom (size $64 \times 64 \times 64$) and the center slices of some reconstructed volumes. Again about 60% of the sinogram data ($N = 256 \times 128$, $\Phi = 225$) was missing. Since the different interpolation methods can easily be extended to 3D and gave qualitatively similar results to the 2D case, we show here only the results for BI interpolation that took 1.5 minutes.

We have seen that it is possible to interpolate missing sinogram data using fast variational techniques to

Method	# Iter.	E_r	α	Time (sec.)
IH	200	9.60	$(0.01, 0.99)$	0.67
BI	1000	9.54	$(0.1, 0.9)$	6.48
IN	300	9.58	$(0.1, 0.9)$	61.39
AH	300	9.52	$(0.1, 0.9)$	2.23
SD	1000	9.93	-	21.02

Table 1. L_2 -norm of the reconstruction error E_r for different interpolation methods.

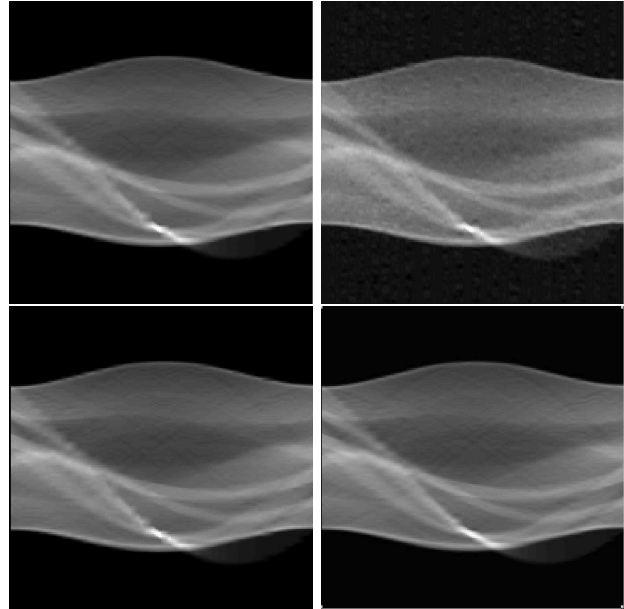


Figure 2. Interpolated sinogram using linear diffusion (TL), SD interpolation (TR), AH interpolation (BL) and BI interpolation (BR).

reduce streak artifacts without blurring important details in the reconstructed images. The next step will be to use this method for real medical datasets.

References

- [1] T. Aach and V. Metzler. Defect interpolation in digital radiography - how object-oriented transform coding helps. *SPIE Procs. Medical Imaging 2001*, 4322:824–835, 2001.
- [2] M. Bertram, G. Rose, D. Schäfer, J. Wiegert, and T. Aach. Directional interpolation of sparsely sampled cone-beam CT sinogram data. In *ISBI*, pages 928–931, 2004.
- [3] M. Buhmann. *Radial Basis Functions*. Cambridge University Press, Cambridge, UK, 2003.

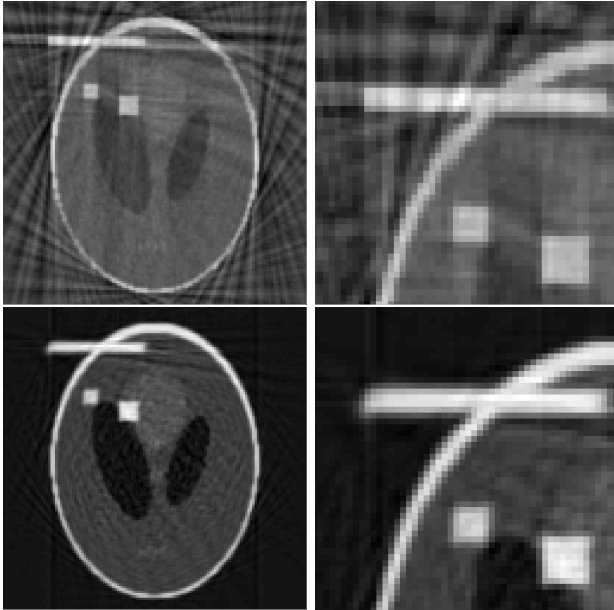


Figure 3. Reconstructed images without interpolation (top) and with BI interpolation (bottom).

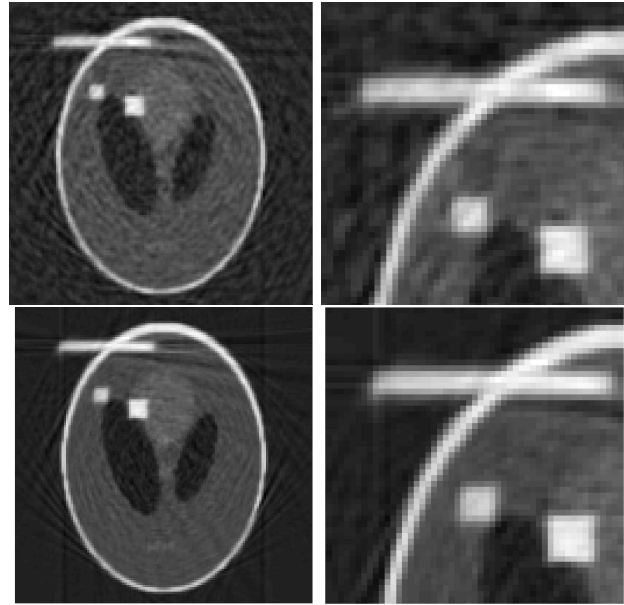


Figure 4. Reconstructed images using SD interpolation (top) and AH interpolation (bottom).

- [4] V. Caselles, J.-M. Morel, and C. Sbert. An axiomatic approach to image interpolation. *IEEE Transactions on Image Processing*, 7(3):376–386, March 1998.
- [5] T. Chan and J. Shen. Non-texture inpainting by curvature-driven diffusions (cdd). *J. of Visual Comm. and Image Representation*, 12(4):436–449, 2001.
- [6] L. Feldkamp, L. Davis, and J. Kress. Practical cone-beam algorithm. *J. Opt. Soc. Am. 1(A)*, pages 612–619, 1984.
- [7] A. Happonen. *Decomposition of Radon Projections into Stackgrams for Filtering, Extrapolation, and Alignment of Sinogram Data*, volume Publication 557. Tampereen teknillinen yliopisto. Julkaisu - Tampere Univ. of Technology, Dep. of Inf. Technology, 2005.
- [8] B. Horn and B. Schunck. Determining optical flow. *Artificial Intelligence*, (17):185–203, 1981.
- [9] J. Prince and A. Willsky. Hierarchical reconstruction using geometry and sinogram restoration. *IEEE Trans. on Image Processing*, 2(3):401–416, July 1993.
- [10] J. Sanz and T. Huang. On the Gerchberg - Papoulis algorithm. *Circuits and Systems, IEEE Transactions on*, 30(12):907–908, 1983.
- [11] U. Trottenberg, C. Oosterlee, and A. Schüller. *Multi-grid*. Academic Press, 2001.
- [12] J. Weickert. *Anisotropic Diffusion in Image Processing*. Teubner, Stuttgart, 1998.
- [13] J. Weickert and M. Welk. Tensor field interpolation with PDEs. In *J. Weickert, H. Hagen (Eds.): Visualization and Processing of Tensor Fields*, Springer, Berlin 2005. to appear.

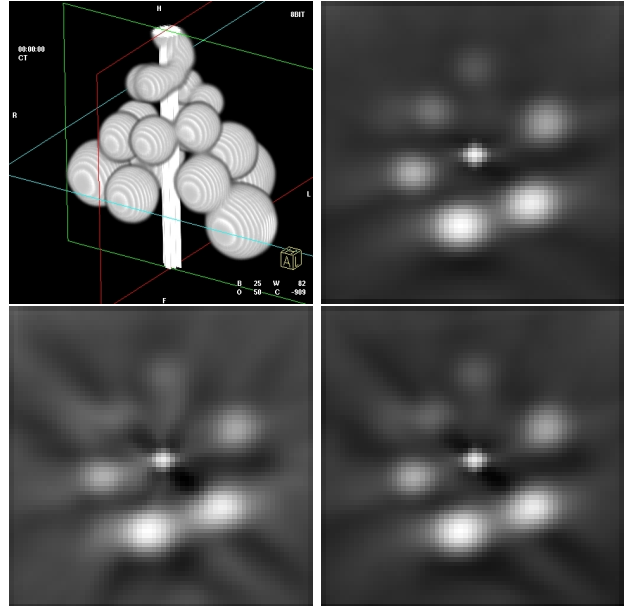


Figure 5. 3D phantom (TL) and center slices of reconstructed volumes using full sinogram (TR), sinogram with gaps (BL) and sinogram interpolated with BI interpolation (BR).